Sensors & Transducers, Vol. 211, Issue 4, April 2017, pp. 23-31

www.sensorsportal.com

Sensors & Transducers

Published by IFSA Publishing, S. L., 2017
http://www.sensorsportal.com

Nanocrystalline $CdSnO_3$ Based Room Temperature Methanol Sensor

Shanabhau BAGUL, Dhanashri PATIL, Priyanka PATIL and * Lalchand PATIL

Nanomaterials Research Laboratory, Department of Physics, Pratap College Amalner. Jalgaon, India
E-mail: plalchand_phy_aml@yahoo.co.in

Received: 16 March 2017 /Accepted: 17 April 2017 /Published: 30 April 2017

Abstract: Synthesis of nanocrystalline $CdSnO_3$ powder by ultrasonic atomizer assisted wet chemical method is reported in this paper. Synthesized $CdSnO_3$ powder was characterized by X-Ray Diffraction (XRD), Field Emission Scanning Electron Microscopy (FESEM) and Transmission Electron Microscopy (TEM) to examine phase and microstructure. FESEM and TEM analysis reveals that the $CdSnO_3$ powder prepared here is porous monodisperse nanocrystalline in nature, with average particle size of approximately 17 nm or smaller. The material is also characterized by UV-Visible and Photoluminescence (PL) spectroscopy. Thick films of synthesized $CdSnO_3$ powder fired at 850 °C are made by using screen printing method. The films surface is modified by using dipping method. $CuCl_2$ (0.005M) dipped (for 2 min) thick film shows high response (R= 477) to 100 ppm methanol at room temperature (35 °C). The sensor shows good selectivity and fast response recovery time to methanol. The excellent methanol sensing performance, particularly high response values is observed to be mainly due to porous $CdSnO_3$ surface.

Keywords: Cadmium stannate, Nanocrystalline powder, Thick films, Methanol sensors.

1. Introduction

In the last 2-3 decades the development of industrial zone uses methanol in many industrial processes, home appliances, as a fuel, and in the production of biodiesel. Volatile organic compounds (VOCs) are easily evaporated at room temperature, which can cause both short-and long-term adverse health effects, such as breathing discomfort, cancers of nervous system, endocrine system and the brain [1-2]. However methanol has strong toxicity and affects on nervous system. Researchers have comparatively more focused on methanol as compare to other volatile organic compounds. Thus it is necessary to develop high response and selectivity methanol gas sensor. Metal oxide semiconductor gas sensors play an important role in environmental monitoring [3].

Metal oxide semiconductor (MOS) gas sensor, as one of the most important conductometric sensors, has attracted dramatic attentions due to their numerous positive features [4-7]. Phase control of perovskite oxides (ABO_3) with a desired composition is still a challenge owing to their various stoichiometries (e.g. typical formulas of ABO_3, A_2BO_4 and AB_2O_4) and the associated complex structures [8-9]. In recent years, considerable efforts have been devoted to the synthesis of these complex metal oxides [10]. More effort is needed to reveal their phase evolution and formation mechanism, which is much important for addressing their properties and technological potentials with a specific phase. It is well-known that the gas sensing characteristics are greatly dependent on its morphology and structure, such as porosity, grain size, surface-to-volume ratio, and morphology. The

$CdSnO_3$ is a perovskite material, which has good thermal and chemical stability due to this it is good candidate for gas sensor. The perovskite and ilmenite cadmium stannate ($CdSnO_3$), have been used as alcohol vapor sensing materials [10-13]. In recent years, cadmium stannate ($CdSnO_3$) used as electrochemical material [14-15]. $CdSnO_3$ have shown quite attractive gas sensitivity properties to various gases such as C_2H_5OH gas [16], chemical warfare agents Chloro Ethyl Sulphonate (CEES) [17-18].

Modification of pure semiconductor metal oxide is another effective and simple way to improve the gas sensing performance by increasing response, selectivity, stability and decreasing the response-recovery time [19-24]. In recent years, some metal oxides and complex metal oxides have been reported to be used as methanol gas sensors [25-34]. But many of those sensors work at high temperature [26-34].

2. Experimental

2.1. Synthesis and Characterization of $CdSnO_3$

Ultrasonic atomization assisted chemical method was used to synthesize $CdSnO_3$ nanoparticles. All the chemicals were of analytical grade and used as-received without further purification. In a typical procedure we took 1.1417 g $CdCl_2.H_2O$ and 1.7528 g $SnCl_4.5H_2O$ were respectively dissolved in 100 ml ethanol (99.9 % purity) to make 0.05 M solution. 0.5 ml hydrochloric acid (HCl) was added drop by drop into the solution of cadmium chloride (0.05 M, 100 ml) called as solution A. $SnCl_4$ solution (0.05 M, 100 ml) was called as solution B. Solution A was mixed into solution B at room temperature with rigorous stirring for 10 min, forming a mixture of solutions called solution C. 5 ml double distil water was added into the mixture solution C. The mixture solution C was ultrasonicated for 60 minute by using ultrasonic atomizer (2.1 MHz Gapusol 9001 RBI Meylan, France). The solution C got transferred from the transparent form to viscous milky. The viscous solution was dried in hot air oven at 80 °C to get white precipitate powder. The powder was collected and fired at 850 °C for 1 hour in muffle furnace.

2.2. Paste Formulation and Preparation of $CdSnO_3$ Thick Films

The thixotropic paste was formulated by mixing the nanocrystalline $CdSnO_3$ powder fired at 850 °C with solvent of ethyl cellulose (a temporary binder) in mixture of organic solvents, such as butyl cellulose, butyl carbitol acetate and turpinol, etc. The ratio of inorganic and organic part was kept at 75:25 in formulating the paste. The paste was screen printed on glass substrates in the desired pattern to obtain the sensors. These sensors were fired at 500 °C for 30 minute to remove the organic binder permanently [35-36]. The films fabricated from as prepared nanocrystalline $CdSnO_3$ powder were termed as 'unmodified $CdSnO_3$ films and referred to as S0 sensor.

2.3. Preparation of Cu-modified $CdSnO_3$ Thick Films

The Cu-modified $CdSnO_3$ thick films were prepared by dipping them into a 0.005 M aqueous solution of Copper chloride $CuCl_2.2H_2O$ for different dipping time intervals of 1, 2, 3, 4 and 5 min and referred respectively as S1, S2, S3, S4 and S5 sensors. The films were dried at 80 °C under IR lamp, followed by firing at 500 °C for 30 min in muffle furnace. These surface modified films were called as 'Cu-modified $CdSnO_3$' films.

2.4. Characterization and Gas Sensor Measurements

The phase and structural study of the powder were determined by powder X-ray diffraction (Bruker D8 Advance) with Cu-Kα1 radiation (λ= 1.5406 A^o) operating at 40 kV, 30 mA at a scanning rate of 2^o of 2θ per minute over the range 20-80^o. The powder was confirmed to be of $CdSnO_3$. The morphology and nanostructure of the prepared thick films were investigated by using field emission scanning electron microscopy (FE-SEM: JSM 670 F, JEOL Tokyo Japan) and transmission electron microscope (TEM) (Philips-CM200) with an acceleration voltage of 200 kV. TEM samples were prepared from depositing a drop of diluted suspension of the as-prepared powders in ethanol on a carbon film-coated copper grid. The chemical composition was investigated by using energy dispersive spectrum (EDAX). The thermal properties of the synthesized powder were analyzed by using thermogravometric-differential scanning calorimetry (TG-DSC) spectrum (STA-6000, Perkin Elmer). The optical properties (band gap) were measured by using ultraviolet-visible spectrophotometer (Shimadzu, Japan) and photoluminescence spectrophotometer (PL, Perkin Elmer). The Fourier transform infrared (FTIR) spectroscopy was used to see the composition of CuO on $CdSnO_3$ thick films.

The gas sensing performance of the $CdSnO_3$ thick films were tested in gas sensing system shown in Fig. 1. The prepared $CdSnO_3$ thick films were cut and made electrical contacts by using purchased silver paste and copper wires. The sensor so fabricated was exposed to various gases mixed with air in chamber. After each exposure to gas, current I_a and I_g was measured by using picoammeter, where I_a and I_g are current flow through the sensor in air and in the test gas respectively. The sensor was exposed to the atmospheric air by opening the chamber.

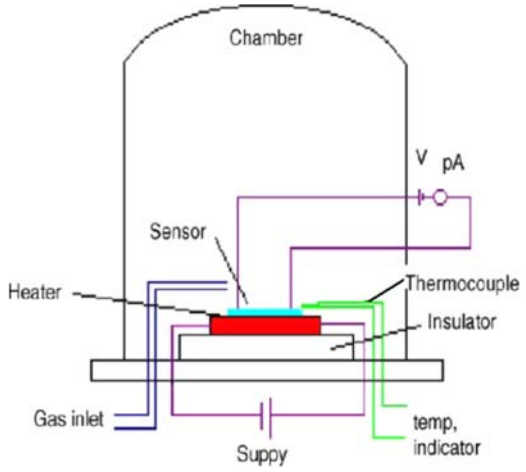

Fig. 1. Block diagram of the gas sensing system.

2.5. Sensing Performance of the Sensors

Gas response (S) of sensor is defined as the ratio of the change in conductance of the sensor on exposure to the target gas to the original conductance in air. It is given as:

$$S = \frac{I_g - I_a}{I_a}, \quad (1)$$

where I_a and I_g are the current flowing through the sensor resistor in air and in a test gas medium respectively. The response time is a time required by the sensor to reach 90 % of its maximum increase in conductance on exposure of the gas. Recovery time is a time required to get back 90 % of the maximum conductance when the flow of gas is switched off.

3. Results and Discussion

3.1. Crystalline Structure and Morphology

The crystalline structure of the as-prepared sample was characterized using XRD. As shown in Fig. 2, the XRD spectra of thick films prepared by powder fired at 850 °C for 1 hour. Fig. 2 shows XRD spectrum of (A) pure $CdSnO_3$ thick film and (B) 2 min dipped ($CuCl_2$) $CdSnO_3$ thick film. All the diffraction peaks of precursor are indexed to the pervoskite $CdSnO_3$ (JCPDS card No. 01-080-3323) without impurity peak. The crystallite size is estimated using the Scherrer formula,

$$D = \frac{0.89\lambda}{\beta cos\theta}, \quad (2)$$

where λ is the wavelength of the X-ray radiation (λ=0.154 nm for $CuK_\alpha 1$) and β is the peak width at half maximum at 2θ, θ is the Bragg diffraction angle, D is the mean crystallite size. Average crystallite size of the prepared sample was approximately 15.23 nm. The TEM images, Fig. 3 also reveals that the particles are of uniform nanospheres with an average diameter of less than 20 nm.

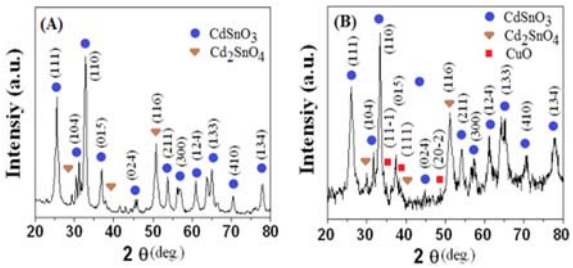

Fig. 2. XRD of thick films of synthesized powder fired at 850 °C (A) Pure, (B) 2 min dipped $CuCl_2$.

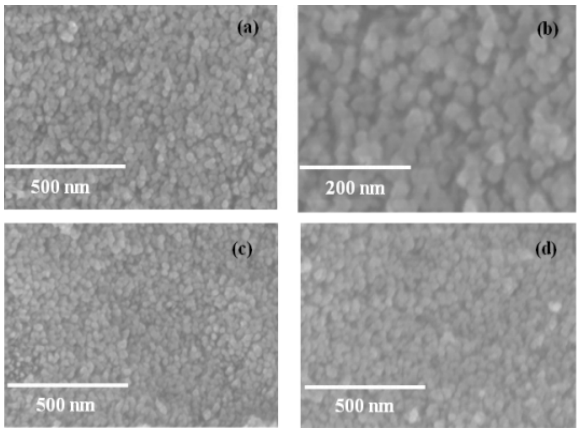

Fig. 3. FESEM images of (a) and (b) pure $CdSnO_3$, (c) 2 min dipped (S2), and (d) 5 min dipped (S5) $CdSnO_3$ thick films.

The morphology and microstructure of the as-prepared samples were characterized using FESEM and TEM. The FESEM image of pure $CdSnO_3$ sample obtained after calcinations is shown in Fig. 3(a), from which a number of uniform nanospheres with an average diameter of 20 nm could be clearly seen. No other morphologies were detected, indicating a high of these nanospheres. Fig. 3(c) and 3(d) shows the FESEM images of 2 and 5 minute $CuCl_2.2H_2O$ (0.005 M) dipped $CdSnO_3$ films respectively. From figures it is seen that the surface get modified with respect to dipping time. The chemical composition of the thick films of pure and surface modified $CdSnO_3$ was measured by EDAX and it is observed that the amount of copper increases with respect to dipping time.

To further investigate the morphology of the as prepared particles, the sample was characterized by TEM. Fig. 4(a)-(c) are TEM images of as obtained nanoparticles. Images possessed elongated nanoparticles having average dimensions less than 20 nm. Fig. 4(d) shows the corresponding selected area electron diffraction (SAED) pattern of prepared powder. Electron diffraction rings reveals the polycrystalline structure of the prepared nanoparticles.

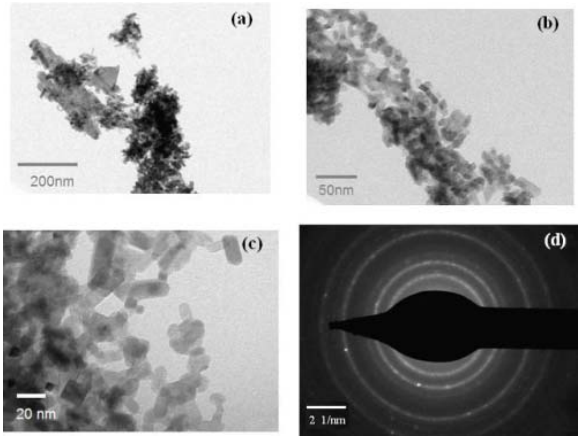

Fig. 4. (a)-(c) TEM and (d) SAED images of the powder fired at 850 °C.

The band gap of as prepare powder fired at 850°C was measured by using UV-Visible spectrophotometer. Fig. 5 shows the UV-Visible absorption spectrum of synthesized $CdSnO_3$ powder. From the absorption spectrum, the band gap was found to be 3.1 eV. The measured band gap value is larger than the standard reported value of 2.9 eV. This blue shift may be occurred due to smaller particle size of $CdSnO_3$.

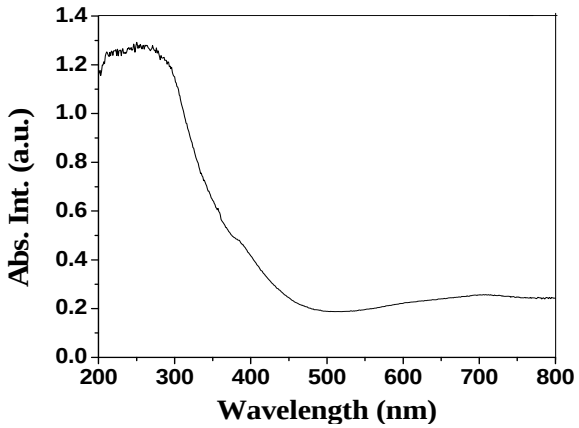

Fig. 5. UV-Visible spectrum of synthesized $CdSnO_3$ powder fired at 850 °C.

The thermogravometric and differential scanning calorimetry (TG-DSC) analysis were carried out in nitrogen atmosphere, heating from 50 °C to 900 °C at the rate of 10 °C/min (Fig. 6). There is first weight loss observed at 100 °C due to the removal of water. At 550 °C the decomposition of chloroethane is take place. The weight loss from 550 °C to 810 °C is due to removal of chloroethane. There is one exothermic peak occur at 840 °C is due to the crystallization of $CdSnO_3$. The balance reaction of as synthesized powder is given in Equation (3).

$$CdCl_2{*}H_2O + 6\ C_2H_5OH + SnCl_4{*}5H_2O = CdSnO_3 + 6\ C_2H_5Cl + 9\ H_2O \quad (3)$$

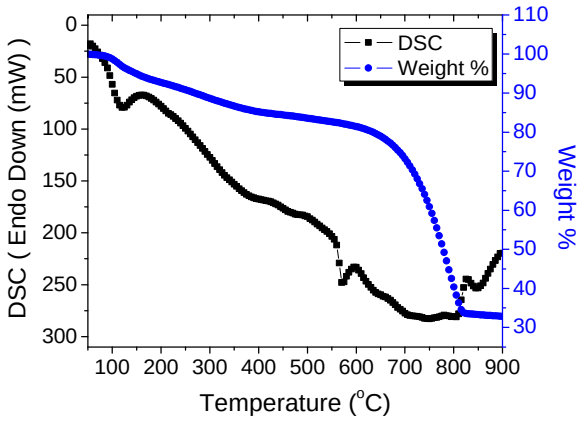

Fig. 6. TG-DSC of synthesized powder.

The defect states in $CdSnO_3$ can be determined by photoluminescence (PL) spectroscopy. The PL spectra of $CdSnO_3$ nanopowder was measured from 350 to 550 nm at room temperature without any filters used in this study (Fig. 7).

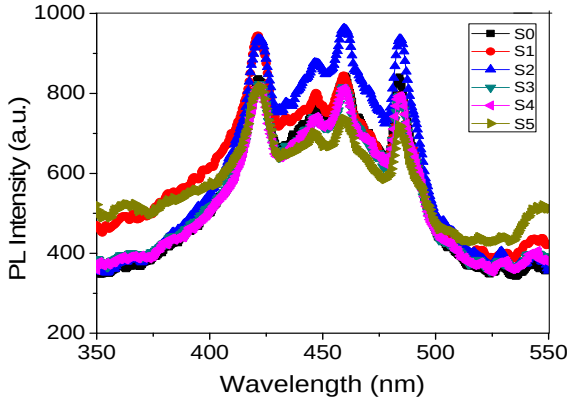

Fig. 7. PL emission spectrum of pure and surface modified $CdSnO_3$ thick films with Exc.300 nm.

Different extrinsic and intrinsic defect centers may be responsible for visible emissions [37-38]. The nanoparticles with large surface to volume ratios have a lot of defects on the surface, which can absorb the O_2^- and O^- ions to form the O_2^-/O^- surface system. Schoenmakers at al [39] have demonstrated that this O_2^-/O^- surface system is the predominant of the electrons in conduction band, which play a key role in the formation of the visible emission centers. Fig. 7 shows emission spectrum of pure and surface modified $CdSnO_3$ thick films with excitation at 300 nm. It is seen from spectrum that the emission intensity of 2 min dipped film is more than that of pure and other dipped films. It may be due to the more heterocontacts form on the surface of film S2 as compare to the others. The photoluminescence energy associated with localized defect levels can be used to identify specific defects and the amount of photoluminescence can be used to determine their concentration.

The amount of copper oxide on surface of dipped $CdSnO_3$ ($CuCl_2 2H_2O$, 0.005 M) thick films were observed by FTIR spectrum (Fig. 8). From FTIR spectrum it is seen that pure $CdSnO_3$ film (S0) do not show CuO peak and other films from S1 to S4 shows CuO peak with increasing absorbance. Peak intensity in infrared spectra shows the concentration of molecules in the sample. From IR spectrum (Fig. 8) it is observed that the amount of CuO increases with dipping time of films in $CuCl_2.2H_2O$ (0.005 M) solution. The surface coverage of $CdSnO_3$ films increases with dipping time, at 2 min dipped films there may be more heterocontacts on the surface as compare to other films.

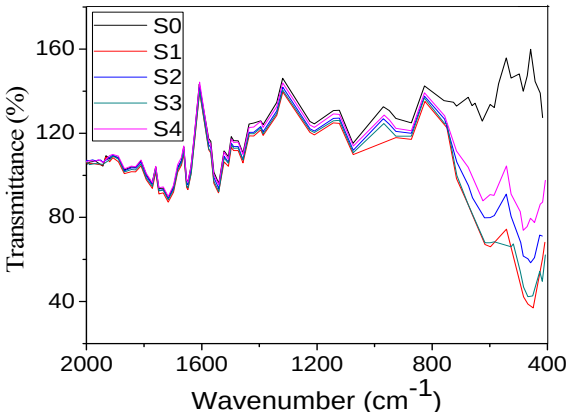

Fig. 8. FTIR spectrum of pure and surface modified $CdSnO_3$ thick films.

3.2. Gas Sensing Properties

Thick films of synthesized $CdSnO_3$ powder were surface modified by using dipping method and made electrical contacts by using purchased silver paste and copper wires. We measured methanol response of pure and surface modified $CdSnO_3$ films. Fig. 9(a) shows the variation of response of sensors to methanol. It is observed that the 2 minute dipped film (S2) gives highest response to 100 ppm methanol at room temperature (35 ºC) as compare to others. At 2 minute dipped film the heterocontacts between CuO and $CdSnO_3$ may be larger as compare to the other films. The amount of Cu on surface was measured by EDAX and it shows the amount increases with dipping time. The methanol is more easily dissociated on heterocontacts as compare to pure $CdSnO_3$. It is known the operating temperature play important role in determining gas sensing performance of the sensor. Thus to determine optimal operating temperature to detect methanol the gas sensing measurement were carried out at different operating temperature to 100 ppm methanol. It is observed from experiment that the sensor S2 shows slowly ascending response from room temperature to 150 ºC and descends very quickly above 150 ºC operating temperature (Fig. 9 (b)).

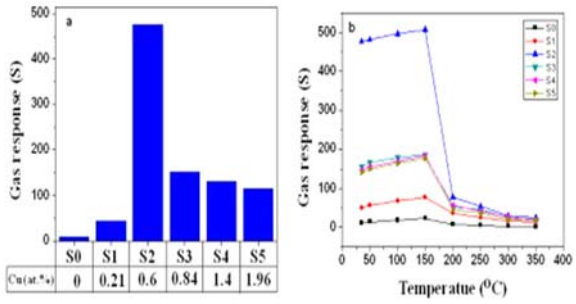

Fig. 9. (a) Response of pure and surface modified sensors to 100 ppm at 35 ºC. (b) Response versus operating temperature of the sensor exposing to 100 ppm methanol.

The selectivity of gas sensors is the ability that a sensor can distinguish different kinds of gases. Selectivity is important gas sensing property. We measure the selectivity of sensor to various gases at room temperature. The $CuCl_2$ dipped (for 2 minute) $CdSnO_3$ thick film (Sensor S2) gives good selectivity to methanol. It can be seen that the sensitivity of sensor S2 to methanol was higher than the sensitivity for other gases at room temperature. Fig. 10(a) shows selectivity of the sensor S2 to various gases.

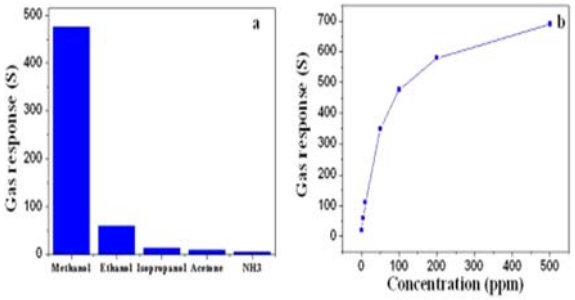

Fig. 10. (a) Selectivity of sensor S2 to 100 ppm vapors at 35 ºC, (b) Response versus methanol concentration of sensor S2 at 35 ºC.

The sensing performance of the sensor S2 to methanol with different concentration was also performed at room temperature (35 ºC). Fig. 10(b) shows methanol response of the sensor S2 tested at various methanol concentrations: 5, 10, 20, 50, 100, 200, 500 ppm at room temperature (35 ºC). From experiments it is observed that the response increases with concentration. At lower concentrations, the response increases fastly and then slowly at higher concentrations of methanol. Stable output of the sensor is important characteristic of sensor for practical application. The experiments to test sensor performance were repeated for few days to study the stability. As seen from experiment (Fig. 11(a)), the long term stability of the sensor has nearly constant response to 100 ppm methanol vapors, which confirmed the good stability of Cu modified $CdSnO_3$ thick film (S2).

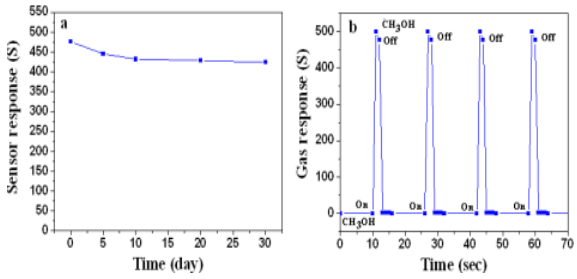

Fig. 11. (a) Stability of sensor S2, and (b) Response recovery curve of sensor S2 to 100 ppm methanol at room temperature (35 ºC).

The response and recovery time is an important factor to evaluate the gas sensing properties of the sensor. The response time was defined as the time required for the variation in resistance to reach 90 % of the equilibrium value after a test gas was injected, and the recovery time as the time necessary for the sensor to return to10 % above the original resistance in air after releasing the test gas. The response recovery time of the sensor S2 to 100 ppm methanol at 35 ºC was measured. It is observed that the sensor response in 2 seconds and recover in 5 seconds. Response and recovery times of the sensor were measured to check repeatability and reproducibility (Fig. 11(b)). The sensor was observed to be reproducible. The sensor S2 exhibited fast response (2 s) and quick recovery (5 s). These values are notable when compared with the response and recovery times reported values by the other researchers (Table 1). The rapid response and recovery of our sensors are due to the porous structure of $CdSnO_3$ nanospheres, the CuO modified $CdSnO_3$ nanospheres based thick film sensor (S2) exhibit excellent reproducibility as four reversible cycles of the response curve maintain their initial response value shown in Fig. 8(b). Furthermore, a comparison of this work and some typical metal oxide gas sensors to methanol is presented in Table 1. It should be pointed that the CuO modified $CdSnO_3$ thick film in present study exhibit higher response and shorter response and recovery time when compared with other metal oxide semiconductor sensors reported in previous works [25-34]. The response of nanocrystalline $CdSnO_3$ thick film sensor S2 to methanol is much higher than the responses reported in literature, as shown in Table 2.

Table 1. Qunatitative elemental analysis.

Element (wt %)	Dipping time (min)					
	0 (pure)	1	2	3	4	5
Cd	22.19	20.09	19.30	18.45	19.53	18.70
Sn	21.31	21.18	20.75	20.16	19.74	20.06
O	56.50	56.12	55.68	55.90	54.20	53.12
Cu	-	2.61	4.27	5.49	6.53	7.58

Table 2. Comparison of the sensing performances of various metal oxide nanostructure-based sensors towards methanol.

Sensing materials	Operating temperature (ºC)	Methanol concentration (ppm)	Sensor response	Response/recovery time (s)	Ref.
$CdSnO_3$ nanoparticles	Room temperature	100	Ra/Rg = 477	2/4	This work
Co_3O_4-intercalated reduced grapheme oxide	Room temperature	800	Rg/Ra = 8.5	240/360	[25]
Ce-doped In_2O_3 nanospheres	320	100	Ra/Rg = 35.2	14/10	[26]
$La_{0.8}Pb_{0.2}FeO_3$ nanoparticles	230	200	Rg/Ra = 50	40/75	[27]
SnO_2-ZnO composite nanofibers	350	500	Ra/Rg = 65	20/40	[28]
ZnO quantum dots	350	100	Ra/Rg = 90	-	[29]
CuO thin films	350	500	(Rg − Ra)/Ra = 0.12	~380	[30]
Al-doped ZnO thin films	275	500	(Ra − Rg)/Ra = 0.44	~280	[31]
CdS-doped SnO_2 thick films	200	5000	Ra/Rg = 70	40/110	[32]
CuO-modified α_Fe_2O_3 hybrid hollow spheres	380	100	Ra/Rg = 14	15/30	[33]
polycrystalline $Cr_{1.8}Ti_{0.2}O_3$ thick films	300	1.2	[(Rg−Ra)/Ra]×100 %=392	23/60	[34]

3.3. Sensing Mechanism

It was observed that the $CdSnO_3$ thick films with surface modified by CuO based sensor shows suddenly decrease in the resistance when the sensor was exposed to reducing gas of CH_3OH, this indicates that the sensor exhibits n-type conductivity behaviors. The experimental results show that the sensing

properties of $CdSnO_3$ were greatly enhanced due to incorporating of CuO. Two main reasons account for these results: first, the nanoparticles of CdSnO3 prepared from ultrasonic atomization offer larger surface accessibility, which will be favorable to adsorption and diffusion of gas molecules, and surface oxidizing reaction of CH_3OH due to the sensing response of semiconductor metal oxide is surface control type [40]. Second the formation of p-n heterojunction at interface between both oxides is responsible for enhancement of gas response [41]. As we know $CdSnO_3$ mainly shows n-type conductivity by electrons and CuO displays p-type conductivity by holes. When the CuO were implanted into the surface of $CdSnO_3$ nanoparticles, the electrons in $CdSnO_3$ and holes in CuO diffuse in opposite direction due to great gradient of the same carrier concentration. Then, the inner electric field was formed at the CuO/$CdSnO_3$ interface and the carriers diffuse was finally balanced [42-43]. As a result, the energy band bends in the depletion layer and the system gets a uniform Fermi level (E_f). This is the formation of p-n junction in equilibrium. When the sensor was exposed to air at room temperature (35 °C), the oxygen molecules adsorbed at the adsorption sites on the surface of the material and form chemisorbed oxygen species. The oxygen species most available at room temperature is O_2^- [44-45] according to Equation (4) and (5).

$$O_2(gas) \rightarrow O_2(ads), \quad (4)$$

$$O_2(ads) + e^- \rightarrow O_2^-(ads) \quad (5)$$

A depletion layer will form on the surface of material, leading to the high resistance state of sensing materials. Moreover, the formation of CuO/$CdSnO_3$ on the surface of $CdSnO_3$, p-n heterojunction with a new depletion layer at their interface also make the resistance of sensor to further increase in air, as shown in Fig. 12.

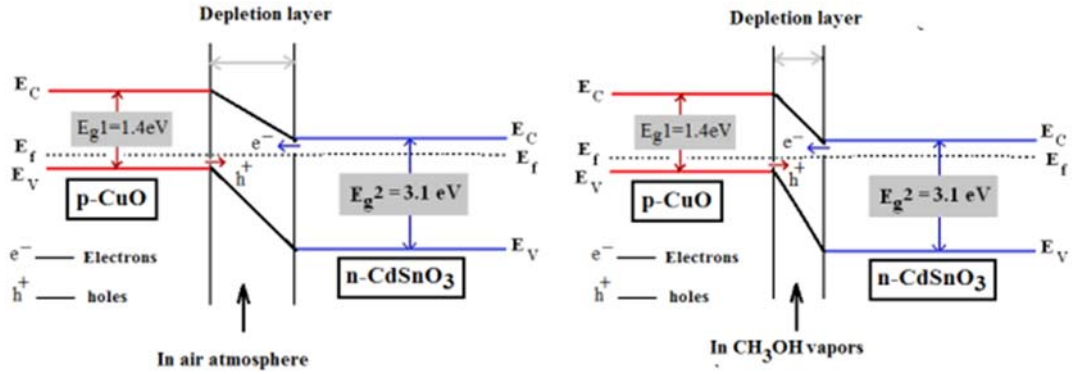

Fig. 12. Schematic diagram for the p-type CuO/n-type $CdSnO_3$ heterojunction based sensor when exposed to CH_3OH vapors.

However, once the composite was exposed to reducing gas of CH_3OH, it reacts with the oxygen species absorbed on the surface of material and release the electrons back to the material as shown in following Equation (6), which decreases the hole concentration in p-type semiconductor of CuO due to electron-hole recombination and reduces the concentration gradient of the same carriers on both sides of p-n junction. Consequently, the depletion layer at the interface becomes thin [46], as shown in Fig. 12. Therefore the resistance of the composite in CH_3OH is further decreased [47], current increases, that is, the sensor response increases according to define $(\frac{I_g - I_a}{I_a})$ of response.

$$CH_3OH + O_2^- \rightarrow CO_2 + 2H_2O + e^- \quad (6)$$

The sensor S2 gives highest response to CH_3OH at room temperature (35 °C) as compared to pure and other surface modified $CdSnO_3$ thick film sensors. This may be due to the large number of heterocontacts are formed between CuO and $CdSnO_3$ on the surface at 2 minute dipped film in 0.005 M $CuCl_2.2H_2O$ solution as compare to other films.

4. Conclusions

$CdSnO_3$ nano particles were synthesized by using ultrasonic atomization assisted chemical method. The morphology and microstructure were analyzed. The $CdSnO_3$ thick films were cupricated by using dipping method. One of the cupricated sensor (S2) shows highest response to methanol at room temperature as compared to pure and other surface modified $CdSnO_3$ thick films. The sensor shows fast response and quick recovery. The sensor gives repeatable performance. It may be concluded that cupricated $CdSnO_3$ thick films may be potential candidate for fabrication of methanol sensor at low cost.

Acknowledgement

Authors thank Pratap College Amalner for providing every facility required to conduct this research.

References

[1]. S. J. Luo, G. Fu, H. Chen, Y. Y. Zhang, Gas sensing properties and complex impedance analysis of La_2O_3-added WO_3 nanoparticles to VOC gases, *Materials Chemistry and Physics*, Vol. 109, Issues 2-3, 2008, pp. 541–546.

[2]. Md. Rajibur Rahaman Khan, B. H. Kang, S. H. Yeom, D. H. Kwon, S. W. Kang, Fiber-optic pulse width modulation sensor for low concentration VOC gas, *Sensors and Actuators B: Chemical*, Vol. 188, 2013, pp. 689–696.

[3]. S. Yi, S. Q. Tian, D. W. Zeng, K. Xu, X. L. Peng, H. Wang, S. P. Zhang, C. S. Xie, A novel approach to fabricate metal oxide nanowire-like networks based coplanar gas sensors array for enhanced selectivity, *Sensors and Actuators B: Chemical*, Vol. 204, 2014, pp. 351–359.

[4]. G. Korotcenkov, Gas response control through structural and chemical modification of metal oxide films: state of the art and approaches, *Sensors and Actuators B: Chemical*, Vol. 107, Issue 1, 2005, pp. 209–232.

[5]. E. Comini, Metal oxide nano-crystals for gas sensing, *Analytica Chimica Acta*, Vol. 568, Issues 1-2, 2006, pp. 28–40.

[6]. N. Barsan, D. Koziej, U. Weimar, Metal oxide-based gas sensor research: how to ?, *Sensors and Actuators B: Chemical*, Vol. 121, Issue 1, 2007, pp. 18–35.

[7]. G. Korotcenkov, Metal oxides for solid-state gas sensors: what determines our choice ?, *Materials Science and Engineering B*, Vol. 139, Issue 1, 2007, pp. 1–23.

[8]. P. V. Vanitha, P. O'Brien, Phase Control in the Synthesis of Magnetic Iron Sulfide Nanocrystals From a Cubane-Type Fe−S Cluster, *Journal of the American Chemical Society*, Vol. 130, Issue 51, 2008, pp. 17256–17257.

[9]. Yi Zeng, Tong Zhang, Huitao Fan, Geyu Lu, Minghui Kang, Synthesis and gas sensing properties of $ZnSnO_3$ cubic nanocages and nanoskeletons, *Sensors and Actuators B: Chemical*, Vol. 143, Issue 1, 2009, pp. 449–453.

[10]. G. Ma, R. Zou, L. Jiang, Z. Zhang, Y. Xue, Li Yu, G. Song, W. Li, J. Hu, Phase-controlled synthesis and gas-sensing properties of zinc stannate ($ZnSnO_3$ and Zn_2SnO_4) faceted solid and hollow microcrystals, *Crys Eng Comm*, Vol. 14, 2012, pp. 2172-2179.

[11]. C. H. Fan, X. Y. Song, H. Y. Yu, Z. L. Yin, H. Y. Xu, G. X. Cao, D. S. Zheng, S. X. Sun, Shape-controlled synthesis of $CaSnO_3$ micro crystals via a precursor route, *Materials Letters*, Vol. 61, Issue 7, 2007, pp. 1588-1591.

[12]. Y. L. Liu, Y. Xing, H. F. Yang, Z. M. Liu, Y. Yang, G. L. Shen, R. Q. Yu, Ethanol gas sensing properties of nano-crystalline cadmium stannate thick films doped with Pt, *Analytica Chimica Acta*, Vol. 527, Issue 1, 2004, pp. 21-26.

[13]. X. H. Jia, H. Q. Fan, X. D. Lou, J. Q. Xu, Synthesis and gas sensing properties of perovskite $CdSnO_3$ nanoparticles, *Applied Physics A: Materials Science & Processing*, Vol. 94, Issue 4, 2009, pp. 837-841.

[14]. Shannon R. D, Gillson J. L, Bouchard R. J, Single crystal synthesis and electrical properties of $CdSnO_3$, Cd_2SnO_4, In_2TeO_6, and $CdIn_2O_4$, *Journal of Physics and Chemistry of Solids*, Vol. 38, Issue 8, 1977, pp. 877–881.

[15]. Sharma Y., Sharma N., Subba Rao G. V., Chowdari B. V. R., Lithium-storage and cycleability of nano-$CdSnO_3$ as an anode material for lithium-ion batteries, *Journal Power Sources*, Vol. 192, Issue 2, 2009, pp. 627–635.

[16]. V. V. Deo, D. M. Patil, L. A. Patil, M. P. Kaushik, Ultrasonically sprayed nanostructured $CdSnO_3$ thin films for the detection of VOC's, *Sensors and Actuators B: Chemical*, Vol. 196, 2014, pp. 489-494.

[17]. L. A. Patil, V. V. Deo, M. D. Shinde, A. R. Bari, M. P. Kaushik, Sensing of 2-chloroethyl ethyl sulfide (2-CEES) - a CWA stimulant - using pure and platinum doped nanostructured $CdSnO_3$ thin films Prepared from ultrasonic spray pyrolysis technique, *Sensors and Actuators B: Chemical*, Vol. 160, Issue 1, 2011, pp. 234-243.

[18]. L. A. Patil, V. V. Deo, M. D. Shinde, A. R. Bari, D. M. Patil, M. P. Kaushik, Improved 2-CEES sensing performance of spray pyrolized Ru-$CdSnO_3$ nanostructured thin films, *Sensors and Actuators B: Chemical*, Vol. 191, 2014, pp. 130–136.

[19]. K. Jain, R. P. Pant, S. T. Lakshmikumar, Effect of Ni doping on thick film SnO_2 gas sensor, *Sensors and Actuators B: Chemical*, Vol. 113, Issue 2, 2006, pp. 823–829.

[20]. Y. Cao, W. Pan, Y. Zong, D. Jia, Preparation and gas-sensing properties of pureand Nd-doped ZnO nanorods by low-heating solid-state chemical reaction, *Sensors and Actuators B: Chemical*, Vol. 138, Issue 2, 2009, pp. 480–484.

[21]. N. D. Singh, C. Y. Yan, P. S. Lee, Room temperature CO gas sensing using Zn-doped In_2O_3 single nanowire field effect transistors, *Sensors and Actuators B: Chemical*, Vol. 150, Issue 1, 2010, pp. 19–24.

[22]. N. Han, X. F. Wu, D. W. Zhang, G. L. Shen, H. D. Liu, Y. F. Chen, CdO activated Sn-doped ZnO for highly sensitive, selective and stable formaldehyde sensor, *Sensors and Actuators B: Chemical*, Vol. 152, Issue 2, 2011, pp. 324–329.

[23]. P. Song, Q. Wang, Z. X. Yang, Preparation, characterization and acetone sensing properties of Ce-doped SnO_2 hollow spheres, *Sensors and Actuators B: Chemical*, Vol. 173, 2012, pp. 839–846.

[24]. N. A. N. Azmy, H. Abdullah, N. M. Naim, A. A. Hamid, S. Shaari, W. H. M. W. Mokhtar, Gamma irradiation effect on the structural, morphology and electrical properties of ZnO–CuO doped PVA nanocomposites thin films for Escherichia coli sensor, *Radiation Physics and Chemistry*, Vol. 103, 2014, pp. 108–113.

[25]. N. Chen, X. G. Li, X. Y. Wang, J. Yu, J. Wang, Z. N. Tang, S. A. Akbar, Enhanced room temperature sensing of Co_3O_4-intercalated reduced grapheme oxide based gas sensors, *Sensors and Actuators B: Chemical*, Vol. 188, 2013, pp. 902–908.

[26]. D. Han, P. Song, S. Zhang, H. Zhang, Q. Xu, Q. Wang, Enhanced methanol gas-sensing performance of Ce-doped In_2O_3 porous nanospheres prepared by hydrothermal method, *Sensors and Actuators B: Chemical*, Vol. 216, 2015, pp. 488–496.

[27]. C. Doroftei, P. D. Popa, F. Iacomi, Synthesis of nanocrystalline La–Pb–Fe–O perovskite and methanol-sensing characteristics, *Sensors and Actuators B: Chemical*, Vol. 161, Issue 1, 2012, pp. 977–981.

[28]. W. Tanga, J. Wang, P. Yao, X. Li, Hollow hierarchical SnO_2-ZnO composite nanofibers with heterostructure based on electrospinning method for detecting

methanol, *Sensors and Actuators B: Chemical*, Vol. 192, No. 1, 2014, pp. 543–549.
[29]. A. Forleo, L. Francioso, S. Capone, P. Siciliano, P. Lommens, Z. Hens, Synthesis and gas sensing properties of ZnO quantum dots, *Sensors and Actuators B: Chemical*, Vol. 146, Issue 1, 2010, pp. 111–115.
[30]. M. Parmar, K. Rajanna, Copper (II) oxide thin film for methanol and ethanol sensing, *International Journal on Smart* Sensing *and Intelligent Systems,* Vol. 4, Issue 4, 2011, pp. 710–725.
[31]. P. P. Sahay, R. K. Nath, Al-doped ZnO thin films as methanol sensors, *Sensors and Actuators B: Chemical*, Vol. 134, Issue 2, 2008, pp. 654–659.
[32]. L. Yadava, R. Verma, R. Dwivedi, Sensing properties of CdS-doped tin oxide thick film gas sensor, *Sensors and Actuators B: Chemical*, Vol. 144, Issue 1, 2010, pp. 37–42.
[33]. Y. Kang, L. Wang, Y. Wang, H. Zhang, Y. Wang, D. Hong, Y. Qv, S. Wang, Onstruction and enhanced gas sensing performances of CuO-modified α-Fe_2O_3 hybrid hollow spheres, *Sensors and Actuators B: Chemical*, Vol. 177, 2013, pp. 570–576.
[34]. S. Pokhrel, L. Huo, H. Zhao, S. Gao, Sol–gel derived polycrystalline Cr1.8Ti0.2O3 thick films for alcohols sensing application, *Sensors and Actuators B: Chemical*, Vol. 120, Issue 2, 2007, pp. 560–567.
[35]. L. A. Patil, A. R. Bari, M. D. Shinde, V. V. Deo, D. P. Amalnerkar, Synthesis of ZnO nanocrystalline powder from ultrasonic spray pyrolysis technique, characterization and its application in gas sensing, *IEEE Sensors Journal*, Vol. 11, Issue 4, 2011, pp. 939–946.
[36]. L. A. Patil, P. A. Wani, S. R. Sainkar, A. Mitra, G. J. Phatak, D. P. Amalnerkar, Studies on 'fritted' thick films of photoconducting CdS, *Materials Chemistry and Physics*, Vol. 55, Issue 1, 1998, pp. 79–83.
[37]. M. W. Ahn, K. S. Park, J. H. Heo, J. G. Park, D. W. Kim, K. J. Choi, J. H. Lee, S. H. Hong, Gas sensing properties of defect-controlled ZnO-nanowire gas sensor, *Applied Physics Letters*, Vol. 93, Issue 26, 2008, pp. 263103-1 – 263103-3.
[38]. N. Han, P. Hu, A. Zuo, D. Zhang, Y. Tian, Y. Chen, Photoluminescence investigation on the gas sensing property of ZnO nanorods prepared by plasma-enhanced CVD method, *Sensors and Actuators B: Chemical*, Vol. 145, Issue 1, 2010, pp. 114–119.
[39]. G. H. Schoenmakers, D. Vanmaekelbergh, J. J. Kelly, Study of Charge Carrier Dynamics at illuminated ZnO Photoanodes, *J. Phys. Chem*., Vol. 100, Issue 8, 1996, pp. 3215-3220.
[40]. D. Ju, H. Xu, Q. Xu, H. Gong, Z. Qiu, J. Guo, *et al*., High triethylamine-sensing properties of NiO/SnO_2 hollow sphere p–n heterojunction sensors, *Sensors and Actuators B: Chemical*, Vol. 215, 2015, pp. 39–44.
[41]. D. Ju, H. Xu, Z. Qiu, J. Guo, J. Zhang, B. Cao, Highly sensitive and selectivetriethylamine-sensing properties of nanosheets directly grown on ceramictube by forming NiO/ZnO PN heterojunction, *Sensors and Actuators B: Chemical*, Vol. 200, 2014, pp. 288–296.
[42]. Y. Chen, L. Yu, D. Feng, M. Zhuo, M. Zhang, E. Zhang, *et al*., Superiorethanol-sensing properties based on Ni-doped SnO_2 p–n heterojunctionhollow spheres, *Sensors and Actuators B: Chemical*, Vol. 166–167, 2012, pp. 61–67.
[43]. S. Bai, W. Guo, J. Sun, J. Li, Ye Tian, A. Chen, R. Luo, D. Li, Synthesis of SnO_2–CuO heterojunction using electrospinning and application in detecting of CO, *Sensors and Actuators B: Chemical*, Vol. 226, 2016, pp. 96–103.
[44]. V. X. Hien, J.-H. Lee, J.-J. Kim, Y.-W. Heo, Structure and NH3 sensing properties of SnO thin film deposited by RF magnetron sputtering, *Sensors and Actuators B: Chemical*, Vol. 194, 2014, pp. 134–141.
[45]. N. Blough, R. Zepp, Reactive oxygen species in natural waters, in: C. Foote, J. Valentine, A. Greenberg, J. Liebman (Eds.), Active Oxygen in Chemistry, *Springer,* Netherlands, 1995, pp. 280–333.
[46]. A. T. Mane, S. T. Navale, S. Sen, D. K. Aswal, S. K. Gupta, V. B. Patil, Nitrogen dioxide (NO_2) sensing performance of p-polypyrrole/n-tungsten oxide hybridnanocomposites at room temperature, *Organic Electronics*, Vol. 16, 2015, pp. 195–204.
[47]. S. Bai, S. Chen, Y. Zhao, T. Guo, R. Luo, D. Li, *et al*., Gas sensing properties of Cd-doped ZnO nanofibers synthesized by the electrospinning method, *J. of Materials Chemistry A*, Vol. 2, Issue 2, 2014, pp. 16697–16706.